The Journal of Experimental Biology 201, 2669–2684 (1998)
Printed in Great Britain © The Company of Biologists Limited 1998
JEB1577

KINEMATICS, MUSCULAR ACTIVITY AND PROPULSION IN GOPHER SNAKES

BRAD R. MOON[1,*] AND CARL GANS[1,2]

[1]*Department of Biology, The University of Michigan, Ann Arbor, MI 48109, USA* and [2]*Department of Zoology, The University of Texas, Austin, TX 78746, USA*

*e-mail: bradmoon@umich.edu

Accepted 13 July; published on WWW 10 September 1998

Summary

Previous studies have addressed the physical principles and muscular activity patterns underlying terrestrial lateral undulation in snakes, but not the mechanism by which muscular activity produces curvature and propulsion. In this study, we used synchronized electromyography and videography to examine the muscular basis and propulsive mechanism of terrestrial lateral undulation in gopher snakes *Pituophis melanoleucus affinis*. Specifically, we used patch electrodes to record from the semispinalis, longissimus dorsi and iliocostalis muscles in snakes pushing against one or more pegs. Axial bends propagate posteriorly along the body and contact the pegs at or immediately posterior to an inflection of curvature, which then reverses anterior to the peg. The vertebral column bends broadly around a peg, whereas the body wall bends sharply and asymmetrically around the anterior surface of the peg. The epaxial muscles are always active contralateral to the point of contact with a peg; they are activated slightly before or at the point of maximal convexity and deactivated variably between the inflection point and the point of maximal concavity. This pattern is consistent with muscular shortening and the production of axial bends, although variability in the pattern indicates that other muscles may affect the mechanics of the epaxial muscles. The kinematic and motor patterns in snakes crawling against experimentally increased drag indicated that forces are produced largely by muscles that are active in the axial bend around each peg, rather than by distant muscles from which the forces might be transmitted by connective tissues. At each point of force exertion, the propulsive mechanism of terrestrial lateral undulation may be modeled as a type of cam-follower, in which continuous bending of the trunk around the peg produces translation of the snake.

Key words: cam, electromyography, gopher snake, kinematics, lateral undulation, locomotion, muscle, *Pituophis melanoleucus affinis*, propulsion, snake.

Introduction

Terrestrial lateral undulation in snakes is effected by muscular activity that produces axial bends and propagates them along the body. The bends form around external objects and exert forces against them; the resulting reaction forces propel the snake forward.

Early studies of undulatory locomotion in snakes resolved the trigonometry of force exertion and the kinematics of terrestrial lateral undulation (Mosauer, 1932*a*,*b*; Wiedemann, 1932; Gray, 1946, 1953*b*; Gray and Lissmann, 1950; Gans, 1962). Gray (1946) first predicted a single pattern of muscular activity and shortening on the basis of the patterns of axial bending. Later, Gray and Lissmann (1950) proposed a variety of muscular activity patterns that could account for the patterns of bending produced during terrestrial lateral undulation. However, Gray and Lissmann (1950) did not discuss the pattern predicted by Gray (1946).

Jayne (1988) recorded muscular activity during terrestrial lateral undulation in two species of slender colubrid snakes (*Elaphe obsoleta* and *Nerodia fasciata*). His results differed substantially from the patterns predicted by Gray and Lissmann (1950). However, Jayne (1988) did not discuss the first prediction of Gray (1946), which closely matched the electromyography (EMG) results. Furthermore, although Jayne (1988) demonstrated that the patterns of epaxial muscle activity were consistent with muscular shortening during lateral undulation, he did not discuss the mechanism by which the active muscles produce curvature or propulsion.

Later, Gasc *et al.* (1989) recorded epaxial muscle activity in the heavy-bodied boid snake *Python regius* during undulation against a single peg. The EMG patterns of the python differed from those predicted by Gray (1946) and Gray and Lissmann (1950) and from those recorded by Jayne (1988) in the colubrid snakes. Gasc *et al.* (1989, based on a personal communication from C.G.) briefly described the propulsive mechanism as a cam-follower system (Fig. 1) based on the principle that ‘a follower on a cam will move from a site of narrow curvature to one of wider radius.’ Gans (1994) and Gans *et al.* (1997) referred to the cam-follower model, but did not expand its analysis. As the cam-follower model is fundamental and more complicated than indicated in the literature, it requires elaboration.

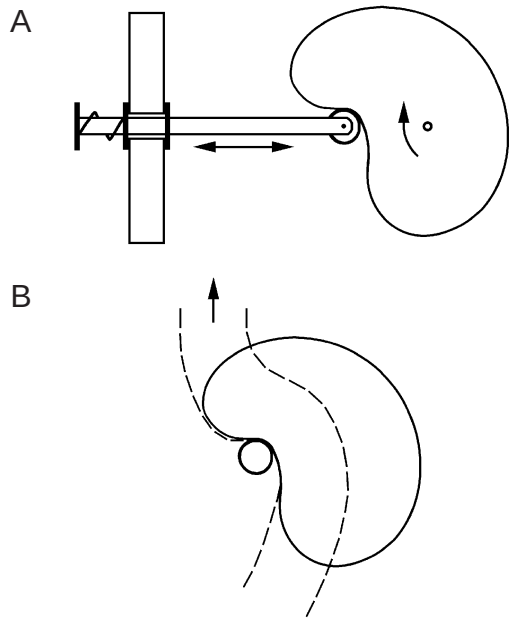

Fig. 1. (A) Schematic drawing of a cam-follower mechanism. The arrows indicate the directions of movement of each element. Rotation of the cam plate induces linear translation of the constrained follower. (B) Terrestrial lateral undulation in snakes modeled as a modified cam-follower mechanism, in which the snake trunk represents an arc of the cam plate and the peg represents a fixed follower. Continuous bending of the snake trunk around the peg, analogous to rotation of the cam plate, produces forward translation of the snake relative to the fixed peg. Additional details are given in the Discussion.

Gasc *et al.* (1989) cautioned that undulation against a single peg was not equivalent to lateral undulation through an array of pegs. In doing so, they implied that the propulsive mechanism used by the python differed from that used by the colubrid snakes studied by Jayne (1988). However, because the python and colubrids studied were moving differently, apparent differences in kinematics, motor patterns and propulsive mechanism remain unresolved. Resolution of these differences requires data on individual snakes performing both kinds of undulation in standardized experiments. Furthermore, testing of the generality of the patterns observed by Jayne (1988) and Gasc *et al.* (1989) requires study of additional species.

In the present study, our major goal was to examine in detail the mechanism by which muscle activity produces curvature, force exertion and propulsion during terrestrial lateral undulation in another species of colubrid snake, the gopher snake (*Pituophis melanoleucus affinis*). To this end, we (1) recorded the kinematic and motor patterns during both kinds of undulation recorded by Jayne (1988) and Gasc *et al.* (1989), (2) tested whether differences in body mass account for the different muscular activity patterns recorded in colubrid and boid snakes, and (3) examined in detail the cam-follower model of undulatory propulsion. The results encompass the kinematics of the entire body and of specific points along the trunk. Consequently, we have identified several novel and critical components in the propulsive mechanism of terrestrial lateral undulation in snakes.

Materials and methods

Specimens and anatomy

For the combined video and electromyographic recordings, we used three specimens of *Pituophis melanoleucus affinis* from southern Arizona, USA (P3, P5, P6), and one specimen from Idaho, USA (P8; Table 1). We used several additional specimens for observations and close-up video recordings. The snakes were housed on a seasonal light cycle and were fed laboratory mice weekly to monthly as needed. The snakes were fasted for at least 1 week prior use in the experiments.

The epaxial muscles of snakes have large cross-sectional areas, long tendons and insertions that suggest that they are important axial flexors (Gasc, 1974, 1981). For these reasons, and to allow comparison with previous studies, we examined the roles of the epaxial muscles. To describe the muscular anatomy and guide the placement of electrodes, we dissected two preserved specimens before the experiments and recorded the lengths and interconnections of the epaxial muscles and their tendons. Subsequently, to confirm the measurements in fresh material, we dissected a third snake after it had been used in the experiments.

Experimental design

We used synchronized videography and electromyography to record kinematic patterns and muscular activity from snakes while they crawled over smooth painted plywood boards. One

Table 1. *Measurements and electrode placements for the four individuals of* Pituophis melanoleucus affinis *used for electromyographic recordings*

Snake	Mass (g)	SVL + TL (mm)	BV + TV	Muscles	Electrode placement
P3	762	1340+160	235+51	SSP, LD, IL	Bilateral V104
P5	703	1145+185	235+61	SSP, LD, IL	Bilateral V90, V91
P6	595	1210+130	236+53	SSP, LD, IL	Unilateral V100
P8	341	970+155	231+61	SSP, LD	Bilateral V25, V75, V125

SVL, snout to vent length; TL, tail length; BV, number of body (trunk) vertebrae from snout to vent; TV, number of tail vertebrae; SSP, M. semispinalis; LD, M. longissimus dorsi; IL, M. iliocostalis; V, vertebra.

board contained a single, foil-wrapped plastic peg, 5 mm in diameter and 60 mm high, in the center. The second board contained an array of nails, 3 mm in diameter and 70 mm high, placed at 15 cm intervals in staggered rows; this board contained a central foil-wrapped plastic peg, as in the single-peg surface. The coefficient of static friction for snake ventral skin being pulled forwards over the painted wood was 0.16–0.20.

Each snake was tested on both peg surfaces for 10–50 trials; snakes that became visibly fatigued or reluctant to crawl were allowed to rest for at least 24 h before further testing. The ambient and surface temperatures under the video spotlights ranged from 20 to 25 °C over several hours of testing different snakes; this slow change in temperature did not appear to affect the locomotor patterns of the snakes.

To test the effects of drag on undulatory kinematics and motor patterns, we subjected snakes to two kinds of increased drag. Snake P3 (unaltered mass 762 g) was induced to pull a 300 g weight attached to the dorsal midline of the tail with tape. On the single-peg substratum used for this experiment, the weight and the peg did not interfere with one another. The weight increased the mass of the snake by approximately 50 % and, therefore, increased the force required for propulsion. Subsequent to the EMG experiments and recovery, snake P5 was tested again while restrained by hand with subjectively greater drag than that of the weight added to snake P3. For snake P5, we measured the curvatures of the body wall and vertebral column directly.

The video and EMG recordings were synchronized using a harness on the snake that sent signals to both the video and EMG tapes. The harness consisted of a thin wire saddle attached at the electrode site and was connected to a 1.5 V battery that formed a circuit upon its brief contact with the foil-wrapped plastic peg. Using this system, contact between the saddle and peg was visible on video tape, and its electrical impulse was simultaneously recorded on the EMG tape.

Kinematics

Experiments were video-taped at 30 frames s^{-1} using a Sony S-VHS video camera. The camera was elevated above the locomotor surface and oriented downwards at approximately 20 ° from vertical.

For video data acquisition, we digitized sequences at 10 frames s^{-1}, which proved adequate for the undulatory movements we recorded (0.02–0.12 m s^{-1}, 0.25–2.09 Hz). We used the MorphoSys program to digitize the body outline in each video frame. We then used custom-written programs to correct for the camera angle, to calculate a finite element midline from each digitized outline and then to calculate rectified curvature (1/radius of curvature) and velocity for each snake.

For the finite element analyses, each computer-calculated midline was divided into 99 equally spaced elements, which corresponded to approximately 2.2 trunk vertebrae per finite element. The entire snake was not visible in every video frame, so velocity was calculated for the tip of the snout. Curvature was measured over arcs of five finite elements (approximately 11 vertebrae) centered on the point of EMG onset at maximal curvature; this approach smoothed the small fluctuations in curvature between adjacent finite elements. This arc length encompassed sufficiently few vertebrae (compared with 22–59 vertebrae in the half-wavelength bend around the peg; see Results) to represent an accurate measure of maximal curvature. Whenever the entire snake was not visible in the video field, we digitized movements of the visible trunk and the position of the electrode through the undulatory cycles.

Muscular activity

We used patch electrodes to record the activity of three epaxial muscles: the semispinalis (SSP) portion of the M. spinalis-semispinalis (SP-SSP), the M. longissimus dorsi (LD) and the M. iliocostalis (IL). Patch electrodes record selectively from single segments within muscle bundles and reduce or eliminate cross-talk from adjacent muscles (Loeb and Gans, 1986). The patch electrodes were made from 0.5 mm thick Dow Corning reinforced Silastic sheeting and 0.11 mm diameter Teflon-coated stainless-steel wire (Medwire, Sigmund Cohn Corp.). The electrode bipole spacing and the bare recording surface of each bipole measured 1.5 mm. The patches ranged in size from 4 mm×4 mm to 4 mm×16 mm and contained one or two electrodes per side. For patches with more than one electrode per side, the inter-electrode spacing was 7.5 mm from center to center of each bipole, which approximated the spacing of muscle segments originating from adjacent vertebrae.

For surgical implantation of the electrodes, the snakes were anesthetized with Halothane using an open-drop method (Bennett, 1996). We made a short longitudinal incision in the skin and underlying fascia and then placed the electrodes into the clefts between the muscle bundles. We placed the electrodes unilaterally or bilaterally between vertebrae 25 and 125 as indicated by ventral scale counts (Alexander and Gans, 1966; Table 1). The electrode wires were held in place with sutures in the fascia and skin and a by small amount of cyanoacrylate glue at the incision. The electrode leads were taped to the dorsal skin at short intervals near the point of implantation; the ends of the lead wires were soldered to Amphenol miniature gold connector pins.

During the experiments, the electrode leads from the snake were connected to amplifier cables suspended approximately 2.5 m from the ceiling, which allowed free movement of the snake with minimal resistance from the cabling. The snakes tolerated the electrodes well for up to 1 week, during which the electrode impedance (measured using the technique of Loeb and Gans, 1986) remained stable. After the experiments, the electrodes were removed surgically and the snakes recovered fully.

The EMG signals were amplified first by Tektronix FM 122 or Tektronix 26A2 differential preamplifiers (gain 1000; bandwidth 100–10 000 Hz) and then by Honeywell 117 direct current amplifiers (gain 1) to stabilize the signal current. Signals from one series of experiments (snakes P3 and P5)

were recorded at 76.2 cm s^{-1} on a Honeywell 5600 14-channel tape recorder (bandwidth 100–10 000 Hz); signals from a second series of experiments (snakes P6 and P8) were recorded at 19.05 cm s^{-1} on a Honeywell 101 medium-band tape recorder (bandwidth 100–2500 Hz).

The EMG data were digitized and analyzed using a DOS-based software package (DataCrunch Software) that contained an A/D signal-acquisition program, a digital finite impulse response filter and an analysis program. The signals were digitized at 8000–10 000 Hz (real time) per channel using a Keithley 12-bit A/D converter, and then digitally filtered below 100 Hz and above 2500 Hz. These sampling rates were sufficient to reproduce accurate EMG spike frequencies and amplitudes (Jayne *et al*. 1990; Moon, 1996). We then calculated the duration (in s), EMG duty factor (burst duration/undulatory cycle duration) and the rectified integrated area (s × V) of individual EMG bursts and analyzed these with the kinematic data.

Analyses

For statistical analyses, we used three specimens of *Pituophis melanoleucus affinis* (P3, P5, P6; Table 1). The fourth specimen (P8) in Table 1 was excluded from the statistical analyses because we recorded from it data for only two of the three epaxial muscles examined in the other snakes. The video and EMG data for the three snakes analyzed statistically comprise EMG bursts from 36 locomotion sequences, of which 14 sequences were from single-peg trials and 22 were from peg-array trials.

To examine the relationships between epaxial muscular activity and kinematics, we used two multiple regression analyses. The regression equations were structured to reflect the appropriate (potential) causal pathways, with kinematic features as dependent variables and measures of muscle activity as independent variables. We coded and analyzed two dummy variables that represented the three individuals (Zar, 1984), and then computed the regressions using centered variables. The simultaneous activity of the three epaxial muscles indicated that they were acting non-independently; furthermore, their forces are probably additive because their combined cross-sectional areas contribute to force production during simultaneous activity. Therefore, for each burst of muscle activity analyzed, we calculated the sum of the rectified integrated areas of the three epaxial muscles (Mm. SSP, LD and IL) and the mean of their durations.

In the first regression analysis, the dependent variable was curvature at the point of EMG onset, and the independent variables were individual (P3, P5, P6), the summed rectified integrated area of the three simultaneous EMG bursts, the mean duration of the muscle bursts and the velocity during the period of muscle activity. We included burst duration in the regression because the same values for area can result from short bursts of large amplitude or long bursts of small amplitude. Although EMG burst area was positively correlated with burst duration (r=0.40, P<0.01), we chose not to scale area by duration using their ratio (area/duration) because of the potential statistical problems associated with using ratios for scaling one variable by another (see Packard and Boardman, 1987, and references therein). In the second regression, the dependent variable was velocity, and the independent variables were individual and the mean duration of the three simultaneous EMG bursts. We excluded the type of peg array from the regressions because a preliminary t-test failed to reveal significant differences (see Results) in curvature between single- and multiple-peg arrays.

We used one-way analyses of variance (ANOVAs) to test for apparent differences in curvature and muscle activity in the first axial bend anterior to a peg, relative to bends at or posterior to the peg. In addition, we used paired t-tests to examine differences in kinematics and muscular activity between freely moving snakes and snakes crawling against increased drag, as described above. With increased drag, a significant increase in EMG burst area in the curve around the single peg would support the inference that the force exerted against the peg is produced by muscles in the axial bend around the peg. Although the tendons of the epaxial muscles are very long, a single wavelength of axial bending usually encompasses one or more complete epaxial muscle–tendon chains (see Results); hence, the results of this test may be used to rule out the contribution of major forces from muscles in axial bends beyond the one in contact with the peg. Potential delays in the timing of excitation–contraction coupling (including time to peak force production and relaxation time) are not likely to decouple EMG signals from force exertion over the extended periods (seconds rather than milliseconds) encompassed by the movements and muscle bursts we recorded. This test of drag also allowed us to determine whether differences in body mass accounted for the differences in the timing of muscle activity between colubrid and boid snakes.

We determined the number of serial muscle segments that were active simultaneously in a bend by multiplying EMG burst duration by velocity and then dividing the product by the length of a mid-trunk vertebra. These calculations allowed us to compare the number of simultaneously active muscle segments in *Pituophis melanoleucus* with those in *Elaphe obsoleta* and *Nerodia fasciata* (Jayne, 1988) and *Python regius* (Gasc *et al*. 1989).

Results

Anatomy

Muscle and tendon lengths vary both among species and within widespread species (Mosauer, 1935; Gasc, 1974, 1981; Pregill, 1977; Jayne, 1982). Our data are for epaxial muscles of the mid-trunk of *Pituophis melanoleucus affinis*, the Sonoran gopher snake, between vertebrae 100 and 130. Muscle terminology corresponds to that of Gasc (1981), and the number of vertebrae spanned by muscle fibers or tendons represents the number of joints spanned by the tissue (i.e. it includes one vertebra of insertion). Each of the epaxial muscles, Mm. spinalis-semispinalis (SP-SSP), longissimus

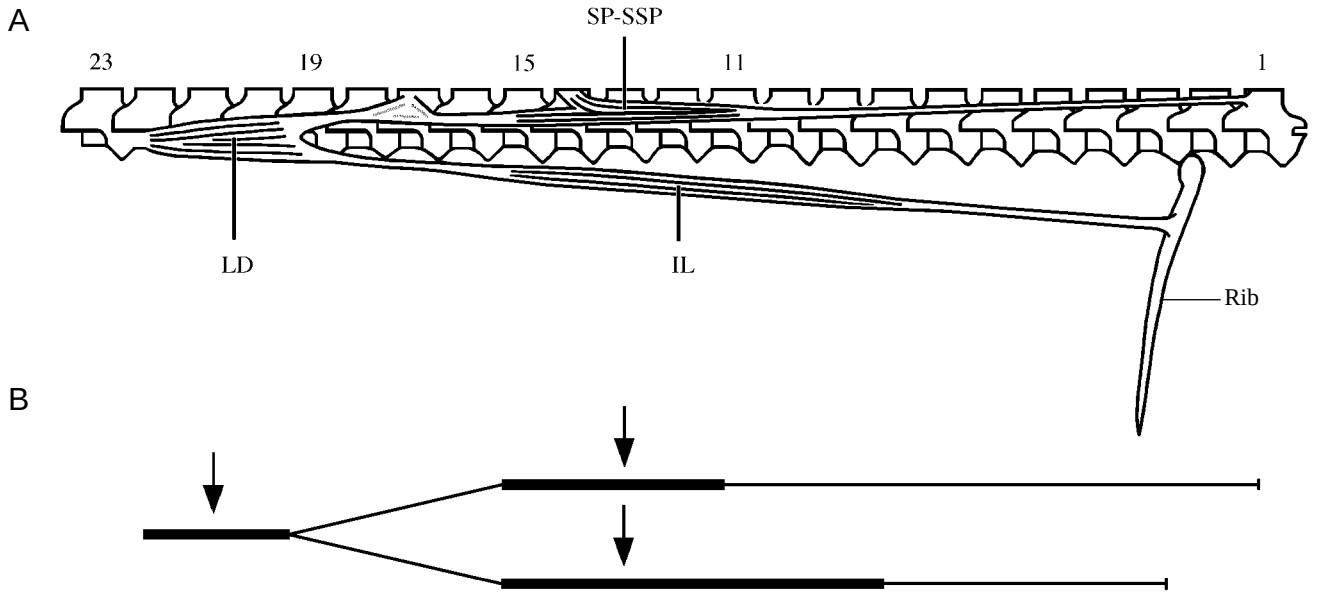

Fig. 2. (A) Epaxial muscular anatomy of the gopher snake *Pituophis melanoleucus affinis*. (B) Diagram of the epaxial musculature and its innervation (indicated by arrows). IL, M. iliocostalis; LD, M. longissimus dorsi; SP-SSP, M. spinalis-semispinalis; numbers indicate vertebral counts from the anteriormost origin of the epaxial muscle–tendon chain. Note that shortening of the SP-SSP and IL would stretch the LD segment that is connected to them by tendons.

dorsi (LD) and iliocostalis (IL) consists of overlapping segments that form a longitudinal column. The muscles are wrapped and their tendons strongly embedded in connective tissue. In addition, the entire musculature is wrapped in a connective tissue sheath that lies deep to the dermis.

The SP-SSP, LD and IL form an interconnected chain of muscle–tendon segments (Fig. 2). The anterior tendon of the SP-SSP forms the anteriormost origin of the muscle–tendon chain. This tendon originates on the dorsal posterior edge of a neural spine and extends posteroventrally for 10 vertebrae to the anterior end of the spinalis-semispinalis fibers. Anteriorly, the SP and SSP are fused, but posteriorly they split. From their common anterior tendon, the SP fibers span three vertebrae posterodorsally and insert on the tendon of the M. multifidis at its origin from a neural spine. The SSP fibers span four vertebrae and are continuous with the anterior (dorsomedial) tendon of the LD. The belly of the SSP is innervated two vertebrae anterior to its origin from the SSP–LD tendon. Posterior to the SSP fibers, the SSP–LD tendon begins as a discrete ribbon, then spreads out to become obscured in the fascia overlying one segment of the SSP column, and then coalesces posteriorly into the discrete anterior tendon of the LD. This tendon spans four vertebrae between the SSP and LD fibers. The fibers of the LD extend posteriorly over four vertebrae and terminate on a vertebral prezygapophysis. The belly of the LD is innervated two vertebrae anterior to its insertion on the prezygapophysis. Overall, the SSP–LD system spans 22 vertebrae from origin to insertion.

The anterior tendinous arch of the LD also gives rise to a ventrolateral tendon that spans four vertebrae anteriorly and connects with the fibers of the IL. The IL extends anteriorly seven vertebrae to insert on an anterior tendon, which spans five more vertebrae and inserts on a rib. The IL belly is innervated two vertebrae anterior to its origin from the LD–IL tendon. From origin (on a rib) to insertion (via the posterior tendon of the LD), the LD–IL system spans 20 vertebrae. Overall, the epaxial muscle–tendon system spans 22 vertebrae and has four insertions on the skeleton.

Kinematics

Initiation of movement

Snakes usually start movement from a stationary position in one of two ways. One pattern, which is often associated with slow speeds, involves a progressive acceleration of the body that begins with the head and proceeds posteriorly. As the head and neck extend forward, successively more posterior parts of the trunk are pulled into motion from a resting position in static contact with the substratum. The moving anterior trunk generally shows some lateral displacement, which brings it into contact with one or more pegs. Once the force exertion exceeds the inertia and static friction of the trunk, the entire posterior trunk is pulled into motion and may engage additional pegs. In this pattern of movement, acceleration initially involves a variant of concertina propulsion, but then shifts to lateral undulation as the trunk engages one or more pegs. During the transition from concertina movement to lateral undulation, both locomotor patterns are used simultaneously along portions of the trunk.

A second pattern of movement involves simultaneous acceleration of the entire trunk. In this pattern, which is often associated with fast starts, lateral undulation begins directly from a resting position. This pattern may occur in the presence

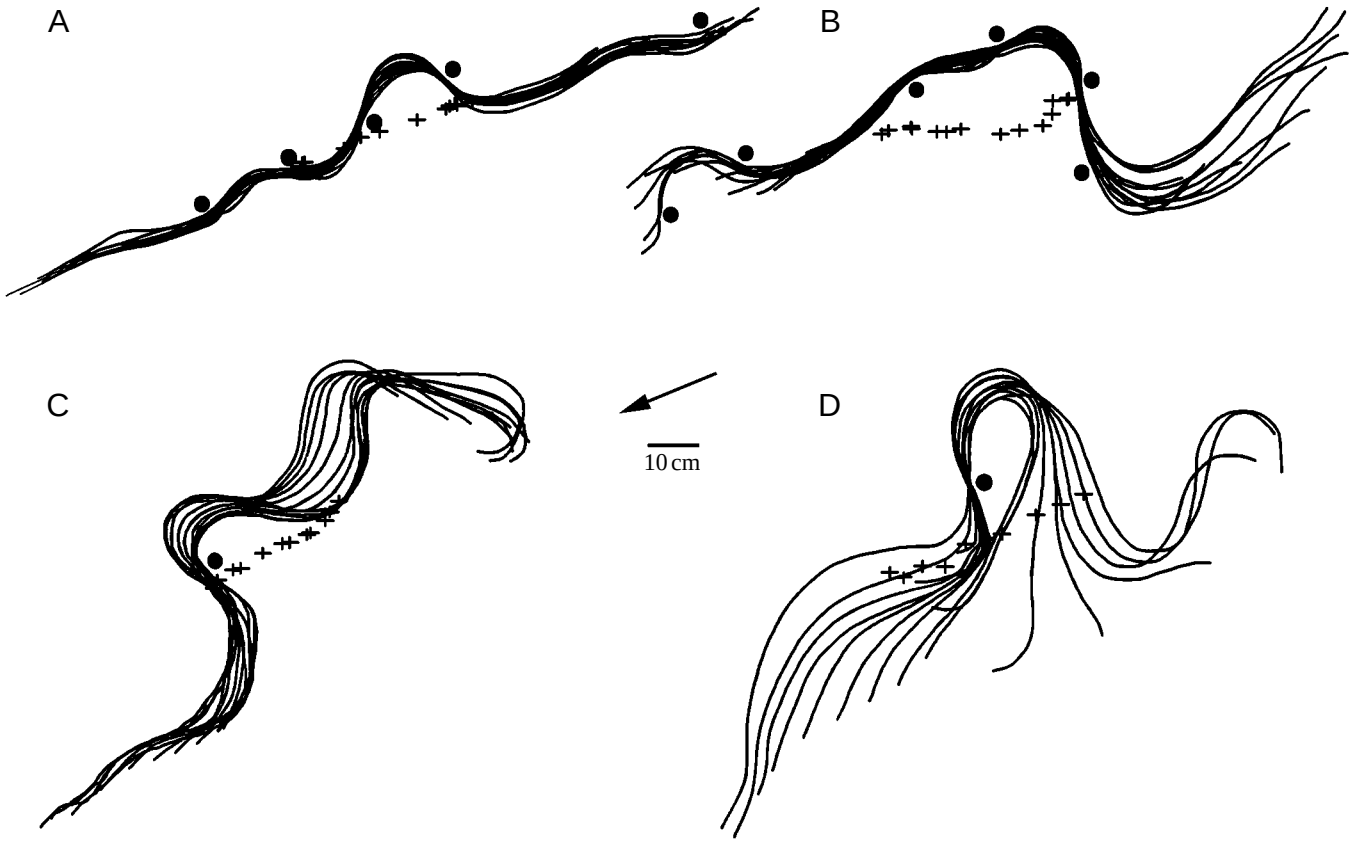

Fig. 3. Successive digitized video frames (10 frames s^{-1}) of *Pituophis melanoleucus affinis* performing typical terrestrial lateral undulation using multiple pegs (A,B) and a more variable undulation by pushing against a single peg (C,D). The arrow indicates the direction of travel for all panels. Forward velocities were 0.05 m s^{-1} (A), 0.06 m s^{-1} (B), 0.05 m s^{-1} (C) and 0.11 m s^{-1} (D). The filled circles represent pegs, and the plus symbols indicate the center of mass for each frame. Note the close contact with the pegs and the steady path of the center of mass, despite the wide swings of the head and tail.

or absence of contact with one or more pegs. In the absence of contact with pegs, rapid movement usually involves substantial posterolateral slippage and thus shifts to slide-pushing. However, whenever movement begins from a stationary position in which the snake is already in contact with one or more pegs, the entire trunk usually begins lateral undulation smoothly with little or no lateral slippage.

Sustained motion

In steady terrestrial lateral undulation, axial bends propagate posteriorly along the body. Therefore, the ventral surface of the trunk is in sliding contact with the substratum and the lateral surfaces are in sliding contact with the resistance sites. Whenever an axial bend contacts a site of resistance, it forms a loose S-shaped curve around the object, with the point of contact at or immediately posterior to the inflection point at which curvature reverses anterior to the peg (Figs 3, 4).

In undulation against a single peg (Fig. 3C,D), the axial bends vary substantially in form and movement, and often incorporate elements of more than one locomotor mode. Contact with the peg is always maintained, as in typical lateral undulation, even though the head and tail often undergo wide lateral slippage, as in slide-pushing. The center of gravity generally follows a smooth line, indicating that the snakes maintain directional control despite the substantial lateral slippage of the head and tail.

Whenever they move through a field of pegs, gopher snakes form curves around several pegs (Figs 3, 4). The head and tail undergo little or no slippage, and the path of the center of mass is closely aligned to the longitudinal axis of the snake (Fig. 3A,B). Each point along the trunk follows the path established by the anterior trunk. Thus, curves travel posteriorly along the body but remain stationary relative to the ground. These standing waves of axial bending are produced and maintained by sequential active bending of the trunk as each segment travels forward through the curved pathway established by the anterior trunk. At some pegs, there is no local postural adjustment and no epaxial muscle activity. These points of contact apparently serve to stabilize the body against lateral slippage, which does not require substantial force exertion. Whenever snakes push against multiple resistance sites, they may stop and restart motion by exerting forces simultaneously against all the resistance sites.

Each half-wavelength bend around a peg contained 22–48

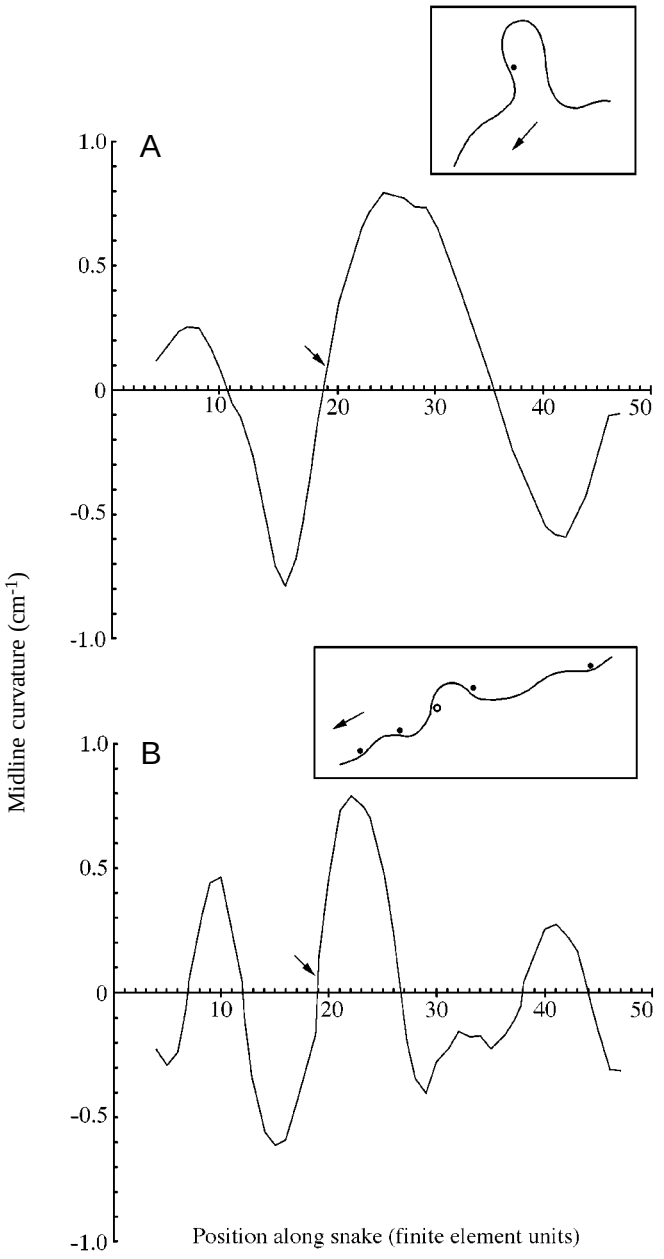

Fig. 4. Midline curvature of *Pituophis melanoleucus affinis* along the trunk for one video frame of movement against a single peg (A) or against multiple pegs spaced 15 cm apart (B). The sequence in A is the same as that in Fig. 3D; the sequence in B is the same as that in Fig. 3A. Curvature is plotted to reflect the orientation of the snakes in the inset panels, so positive curvature indicates convexity on the right side of the snake. On the horizontal axis, 0 is the head and 50 is the tip of the tail. The inset frames indicate the midline from which each curvature plot was generated; the arrow in each inset panel indicates the direction of travel. The arrow on each curvature plot indicates the point of contact between the electrode-bearing segment and the single (A) or central (B, open circle) peg.

vertebrae for gopher snakes in the array of pegs, and 31–59 vertebrae in snakes pushing against a single peg. Curvature of the body around the single peg appeared to be greater than that around any individual peg in the peg array. However, midline curvature at the point of epaxial muscle activation did not differ significantly between single- or multiple-peg substrata (independent t_{198}=–1.89, P=0.06). In the combined sample of snakes pushing against single and multiple pegs, rectified midline curvature at the point of muscle activation ranged from 0.02 to 2.18 cm^{-1} (0.75±0.46 cm^{-1}; mean ± S.D., N=201). Peak midline curvature was not significantly correlated with velocity, EMG burst area or burst duration, although individual snakes varied significantly in the relationships among these variables (Table 2).

Table 2. *Results from the multiple regression of kinematic variables against muscle activity variables for* Pituophis melanoleucus affinis *during terrestrial lateral undulation*

Dependent variable = curvature; N=48

		Standardized partial regression coefficients for independent variables				
Overall adjusted r^2	Overall $F_{5,43}$	EMG burst area	Velocity	EMG burst duration	Individual d1	Individual d2
0.19	3.27*	–0.25	–0.21	0.15	0.65*	0.36

Dependent variable = velocity; N=62

		Standardized partial regression coefficients for independent variables		
Overall adjusted r^2	Overall $F_{3,59}$	EMG burst duration	Individual d1	Individual d2
0.37	13.06**	–0.38**	–0.18	0. 83**

*P<0.05; **P<0.01.

The F value from the regression ANOVA is subscripted with regression and residual degrees of freedom.

EMG burst area and duration are described in the text; d1 and d2 indicate the dummy variables that represent individual values.

Peak midline curvature tended to be lower (0.65±0.33 cm^{-1}; mean ± S.D.) in the first bend anterior to a peg than it was in bends at or posterior to the peg (0.91±0.60 cm^{-1}), although this difference was not significant (ANOVA $F_{2,192}$=2.25, P=0.11). The slightly lower curvature anterior to the peg is associated with a shift in muscle activity (described below) in this bend.

Close-up observations and video recordings indicated that the body wall forms a short-radius curve around the peg and an outward bulge immediately anterior to the peg (Fig. 5). The large-radius bend of the vertebral column and the short-radius bend of the concave body wall represent arcs of two concentric circles. Consequently, the inner body wall would be expected to have a smaller radius of curvature (i.e. greater curvature) than the vertebral column; the difference in radius of curvature would be equal to the transverse radius of the snake trunk. For unrestrained movement of snake P5, the peak curvature of the body wall (measured over intervals of three vertebrae) around

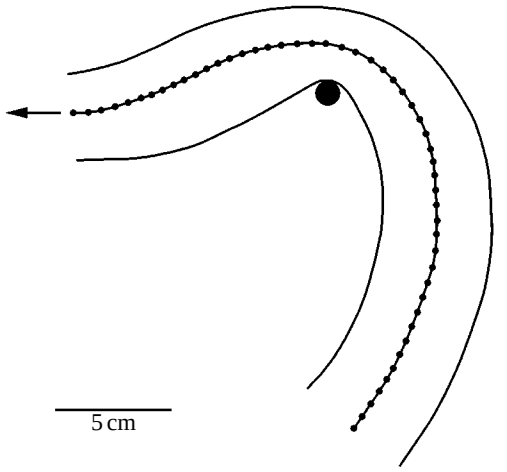

Fig. 5. Differential curvature of the vertebral column (dotted line) and concave body wall in a 50 vertebra section of *Pituophis melanoleucus affinis* bending around a single peg, digitized from a close-up video image in which the vertebral midline was painted for greater visibility. Dots delimit the vertebrae; the arrow indicates the direction of travel.

a single peg was significantly greater than that expected given the observed vertebral curvature and the radius of the trunk (paired t_7=–4.41, P<0.01). The positions of peak vertebral and body wall curvature did not differ relative to one another along the body (paired t_7=–0.38, P=0.72). In three freely moving snakes (P5, P12, P18), the mean curvature of the body wall for three ribs in contact with the peg was significantly greater than that of the body wall immediately posterior to the peg (paired t_{18}=–8.34, P<0.001).

Locomotor kinematics varied in response to different loads imposed on the snakes. When snake P3 was induced to pull a 300 g weight, velocity decreased significantly (paired t_7=3.87, P<0.01) compared with that of free movement. Midline curvature at the point of epaxial muscle activation did not differ significantly from that of free movement (paired t_{10}=1.53, P=0.16). However, when snake P5 was restrained by hand with subjectively greater drag than that of a 300 g weight, curvature around a single peg increased significantly in both the vertebral column (paired t_7=–4.15, P<0.01) and body wall (paired t_7=–5.95, P<0.001) compared with the values during free movement. Furthermore, under the restraint, the position of peak curvature of the body wall shifted posteriorly by a mean of two vertebrae (paired t_7=–2.50, P=0.04) relative to that of the vertebral midline.

The shift in position of midline and body wall curvature appeared to be due to axial torsion in the bends around the peg. In close-up video recordings of a dorsal view, this twisting appeared as progressive lateral displacement of the painted vertebral midline towards one side of the body. Measurements of this displacement indicated that axial bending around points of force exertion involved axial torsion of 1–24° over 10 vertebrae, which is equivalent to 0.1–2.4° per vertebral joint. This torsion appears to contribute to the local deformation of the body wall around each peg: on approach to a peg, the vertebral midline twisted towards the side of contact; on leaving the anterior side of the peg, it twisted away from the side of contact. As a result of this twisting, the ventrolateral body wall is pulled inwards before contact with the peg, and then extended outwards and lifted slightly off the substratum anterior to the peg.

The mean velocity for each period of muscle activity ranged from 0.02 to 0.12 m s^{-1}, and the frequency of undulation ranged from 0.25 to 2.09 Hz. Higher velocities were observed occasionally (e.g. 0.20 m s^{-1} in snake P8; see Fig. 7), but were not represented in the regression data. Velocity was significantly and negatively correlated with EMG burst duration, although individuals differed significantly in this relationship (Table 2).

Muscular activity

Concertina acceleration involved sequential recruitment of epaxial muscles as local portions of the trunk were pulled into motion. However, simultaneous acceleration of the entire trunk, as in lateral undulation, involved simultaneous and coordinated activation of muscles in multiple propulsive bends along the trunk.

During steady lateral undulation, the epaxial muscles were active in unilateral bursts that passed posteriorly along the trunk of the snake and alternated between the sides of the body (Figs 6, 7). The SSP, LD and IL became active just before or at the point of maximal convexity, remained active as they traveled forward past the peg, and ceased activity variably between the inflection of curvature and the point of maximal concavity (Table 3; Fig. 8). The muscles were always active contralateral to the site of peg contact (Fig. 6). In the regression analyses, EMG burst area was not significantly related to midline curvature, whereas burst duration was significantly and inversely correlated with velocity (Table 2).

During undulation against one or more pegs, 1–25 epaxial muscle segments were active simultaneously (7.66±4.56

Table 3. *Timing and duty factor of epaxial muscle activity during terrestrial lateral undulation in* Pituophis melanoleucus affinis

Muscle	Onset phase	Offset phase	Duty factor
SSP	0.21±0.06	0.59±0.10	0.37±0.12
LD	0.20±0.07	0.50±0.12	0.30±0.13
IL	0.22±0.06	0.50±0.12	0.36±0.12
All	0.21±0.06	0.56±0.12	0.34±0.12

Values are means ± S.D.

EMG onset and offset timings are expressed as phase of locomotor cycle, where zero indicates straight posture, 0.25 indicates maximal convexity and 0.50 indicates the subsequent straight posture.

Duty factor indicates EMG burst duration as a proportion of a single undulatory cycle.

For each muscle, N=3 snakes and 13 muscle bursts.

Muscle abbreviations as in Table 1.

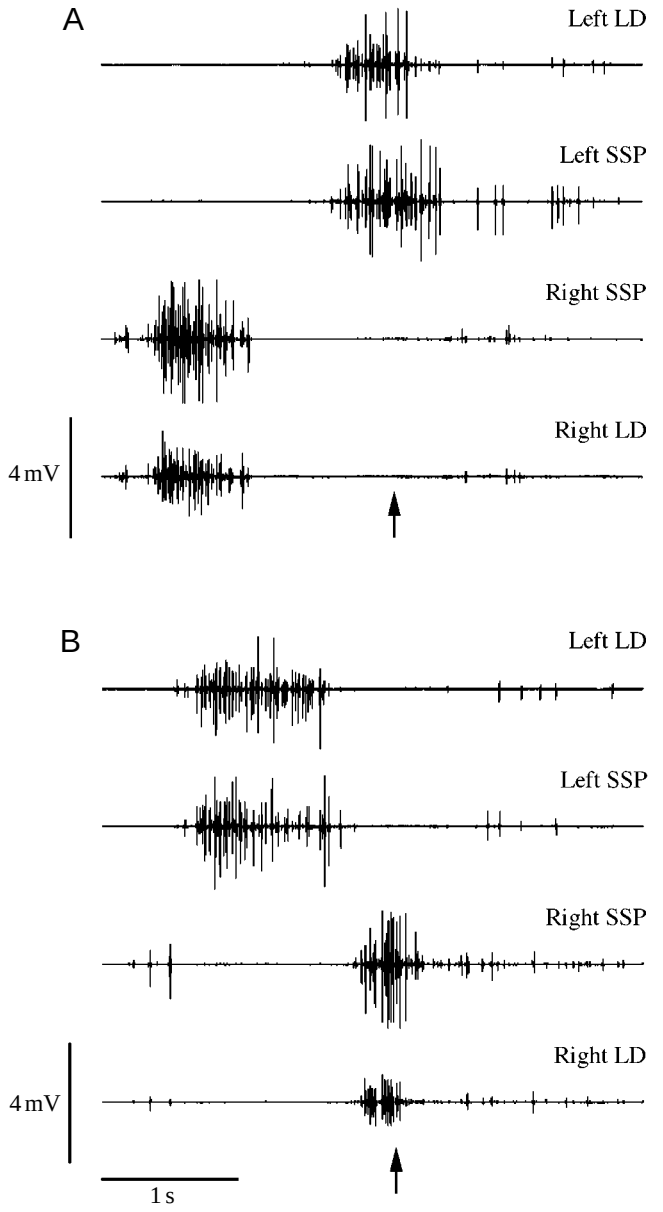

Fig. 6. (A) Epaxial muscle activity in *Pituophis melanoleucus affinis* crawling freely at 0.06 m s^{-1} and pushing against a single peg in a rightward bend. (B) Epaxial muscle activity in the same snake pulling a 300 g weight while pushing against a single peg at 0.03 m s^{-1} in a leftward bend. Muscle activity is attenuated in the bend immediately anterior to the peg in both sequences. Note the silent periods between the offset of activity on one side and the onset of activity on the other side, and the low-level bilateral activity anterior to the point of contact with the peg. Also note the increased electromyogram (EMG) duty factor and the shorter silent period between contralateral EMG bursts with the extra weight. LD, M. longissimus dorsi; SSP, M. semispinalis. The arrow indicates the time of contact between the electrode-bearing segment and the peg.

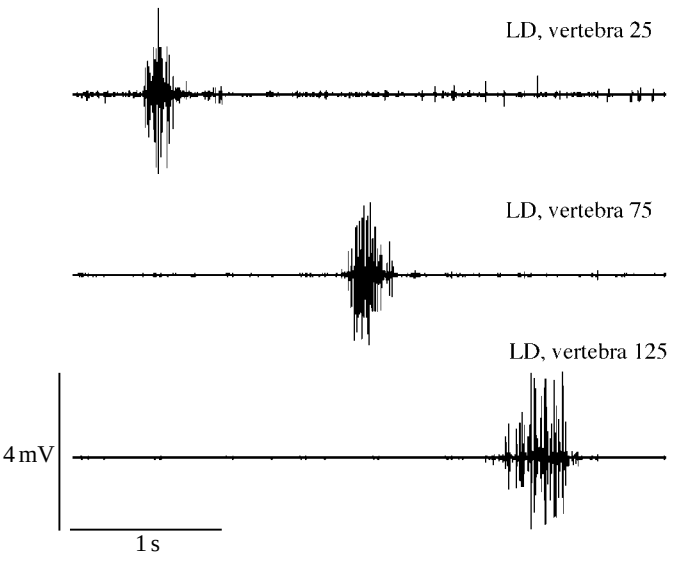

Fig. 7. Longitudinal propagation of activity in the left M. longissimus dorsi (LD) of *Pituophis melanoleucus affinis* pushing against a single peg and moving at 0.20 m s^{-1}.

muscle segments; mean ± S.D., N=221) along one side of the body. Therefore, up to three complete, adjacent chains of SSP–LD–IL muscles were active in each axial bend. Furthermore, for most of an EMG cycle, the active epaxial muscles act over more vertebrae (approximately 8–24) anterior to the peg than posterior to it (approximately 0–14 vertebrae), calculated by counting the number of vertebrae spanned by a single muscle–tendon chain from the point of SSP and IL activation to the deactivation of the LD.

The shift of muscle activity between sides involved a variable delay of 0–0.84 s (0.29±0.24 s; mean ± S.D., N=66), which corresponds to a length of 0–9 vertebrae (2.75±2.41 vertebrae; mean ± S.D., N=66). The shift to contralateral activity was occasionally immediate, and rarely involved up to 0.1 s (one segment) of bilateral muscle activity. Although epaxial muscles are active unilaterally in *Pituophis melanoleucus affinis*, the insertions of active muscles on one side overlap the active fibers of more anterior contralateral muscles by 6–22 vertebrae (see Fig. 10).

In our sample, summed epaxial muscle burst area was significantly smaller in the first bend anterior to the peg from that in bends posterior to the peg (ANOVA $F_{2,60}$=9.36, P<0.001). This difference corresponded to the slightly, but not significantly, lower midline curvature in the first bend anterior to the peg relative to the curvature of bends around or posterior to the peg. This EMG–curvature relationship was anomalous relative to that of other bends. Exclusion of these data from the first regression analyses did not affect the results. In contrast to EMG magnitude, burst duration did not differ significantly among curves along the trunk (ANOVA $F_{2,218}$=0.85, P=0.43).

The attachment of a 300 g weight to snake P3 increased the drag of the animal and, consequently, increased the amount of force required for effective propulsion. The addition of the weight led to significant increases in (1) the summed epaxial EMG rectified integrated area (paired t_6=–5.69, P<0.01), (2) mean burst duration (in s) (paired t_9=–2.64, P=0.03), and (3) the number of simultaneously active muscle segments (paired

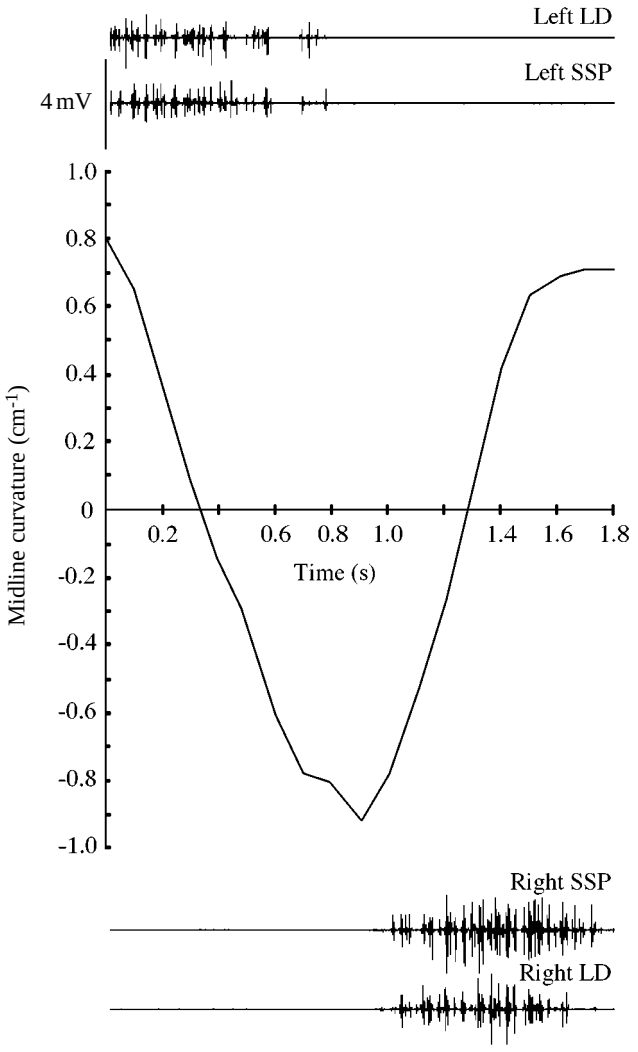

Fig. 8. The relationship between epaxial muscle activity and the curvature of the electrode-bearing segment through time during lateral undulation at 0.03 m s^{-1} in *Pituophis melanoleucus affinis*. Curvature is plotted to reflect a dorsal view of the snake moving to the right, so positive curvature indicates convexity on the left side of the snake. The muscle activity is aligned with one propulsive wavelength of curvature to indicate electromyogram (EMG) onset and offset times relative to axial bending. LD, M. longissimus dorsi; SSP, M. semispinalis.

t_5=–4.40, P<0.01). The mean delay between EMG offset on one side and onset on the other side decreased significantly (paired t_5=5.05, P<0.01) with the addition of the weight. Mean EMG duty factor increased significantly from 0.33±0.13 (mean ± S.D., N=26) in free movement to 0.45±0.05 (N=12; independent t_{35}=–4.15, P<0.01) when pulling the weight. However, maximum EMG spike amplitudes did not change with the addition of the weight (paired t_6=–2.26, P=0.06).

The larger gopher snakes in our sample (approximately 700 g) needed to exert forces of approximately 1.5 N to overcome inertia and static friction and propel themselves freely on the substrata we tested. However, when pulling against calibrated Pesola scales, three 600–700 g gopher snakes could exert much greater maximum pulling forces of 37–45 N.

Discussion

Kinematics

In terrestrial lateral undulation, snakes form axial bends around objects on the substratum. The bends propagate posteriorly along the trunk, pushing against the objects and consequently propelling the snake forward. The degree of curvature around each object (peg) appears to relate to the overall force required for progression (Gray and Lissmann, 1950; Gray, 1953*b*). Gray and Lissmann (1950) noted that the degree of curvature varies inversely with the number of pegs contacted. They also noted that, although overall force exertion increases with the number of pegs contacted, the longitudinal force vector remains relatively constant for a given snake and substratum. These observations indicate that curvature is modulated to control the direction and degree of force exertion against each peg (Van Leeuwen, 1927; Mosauer, 1932*a*,*b*; Gray and Lissmann, 1950; Gasc *et al*. 1989).

In gopher snakes pushing against single or multiple pegs, the vertebral column bends broadly around the peg, whereas the body wall bends sharply and deforms asymmetrically around the anterior surface of the peg (Fig. 5). Thus, the vertebral column and body wall bend differently around each peg. This difference in curvature between the vertebrae and body wall appears to be produced by a combination of three components: a reversal of curvature anterior to the peg, abduction of the body wall in this region and axial torsion. From our data, it is unclear whether movement of the body wall is produced actively by the ribs and their muscles or passively by compression and rebound of the body wall as each segment pushes against the peg and then slides out of contact with it. Local deformation of the body wall and the potential role of the ribs in this movement are consistent with the hypothesis of Gasc (1967, 1974) that the M. levator costa contributes to axial bending and locomotor movements.

Axial twisting in gopher snakes and pythons (Gasc, 1974, 1976) may be due to two non-exclusive factors. First, the twisting may reflect actual torsion at the vertebral joints. Although the zygosphene–zygantrum articulations of snake vertebrae severely restrict torsion, even 1–2 ° of twisting at each joint (Gasc, 1974, 1976) would sum over 22 vertebrae (the lowest number we calculated for a half-wavelength bend around a peg) to produce substantial overall torsion of 22–44 °. This range encompasses the degree of axial torsion we observed in gopher snakes. Second, some torsion could be produced by a combination of lateral bending and lifting of the bends (Gans, 1970, 1974; Gans and Mendelssohn, 1972; Gasc, 1974, 1976). Although we observed slight lifting of the ventrolateral body wall in convex bends, we did not observe substantial lifting of the vertebral column in gopher snakes.

Individuals of *Elaphe quadrivirgata* and other species (Stradling, 1882; Fokker, 1927; Hirose, 1993) may also lift the ventrolateral body wall off the substratum in convex bends. In

addition to its potential role in producing torsion, this 'sinus lifting' of axial bends may enhance locomotor force exertion (Hirose, 1993).

The importance of local deformation of the snake trunk around pegs was noted by Gans (1974) and Cundall (1987), although they did not report the different deformations of the vertebral column and body wall. In *Python regius*, the body wall deforms locally around a peg as a result of activity of the hypaxial musculature (Gasc *et al*. 1989). This local deformation allows finer control of the direction of force exertion than does vertebral curvature alone (Gasc *et al*. 1989). Therefore, reversal of curvature anterior to the peg, differential curvature of the vertebrae and body wall, and axial torsion appear to be critical elements of the propulsive mechanism.

Gray (1946) argued that asymmetry of the curves is a critical element of terrestrial lateral undulation in snakes. Hirose (1993) also noted that, during undulation over plastic turf, *Elaphe quadrivirgata* forms asymmetric curves. Hirose (1993) described the curvature as a 'serpenoid curve' and modeled it mathematically on the basis of a first-order Bessel function. Ostrowski and Burdick (1996) further analyzed the motion described by Hirose (1993) and highlighted the resemblance of the mathematically determined patterns to the movements of snakes. However, the models of Hirose (1993) and Ostrowski and Burdick (1996) do not account for differential curvature of the vertebral column and the body wall, which appears to be a critical component of the propulsive mechanism of lateral undulation in snakes. In the present study, it was unclear whether *Pituophis melanoleucus affinis* bends the vertebral column asymmetrically (which would be reflected in the change of curvature, rather than in its magnitude, along arcs of the body), although the body wall clearly bends asymmetrically around sites of force exertion.

Snake movement may simultaneously involve more than one locomotor mode in different regions of the body (Gans, 1962). Gopher snakes pushing against a single peg always maintain the point of contact with the peg, even though the head and tail may slip laterally over the substratum (Fig. 3). Thus, the head and tail exhibit movements typical of slide-pushing (Gans, 1984), whereas the region pushing against the peg always maintains the curvature pattern of typical lateral undulation. Similarly, in an array of pegs, the snakes maintain simultaneous contact with several pegs. However, the snakes also contact and slide past some pegs in an array without locally adjusting the body wall around them. Presumably snakes detect such pegs with sensory receptors in the skin (Proske, 1969) and use the pegs to prevent lateral slippage, but do not exert much force against them.

Muscular activity

Concertina acceleration from static contact involves sequential recruitment of epaxial muscles as bends of the trunk are pulled into motion. Undulatory acceleration from rest involves simultaneous and coordinated activation of muscles in all bends along the trunk. In steady movement, muscle activity appears to become entrained by the bending pattern around each contact point.

In terrestrial lateral undulation, waves of epaxial muscular activity propagate posteriorly along the trunk (Jayne, 1988; Gasc *et al*. 1989; present study). In *Pituophis melanoleucus affinis*, the timing of muscle activity is consistent with muscular shortening and the production of axial bends: muscles are activated just before or when they become maximally stretched and deactivated when they reach resting length or are maximally shortened. Activation of the muscles just before the point of maximal convexity (Table 3) indicates that the muscles are active briefly while still lengthening, which probably enhances their force production (Katz, 1939; Gordon *et al*. 1966). This pattern of muscle activity is consistent with the point of muscle activation predicted by Gray (1946) and recorded by Jayne (1988) in other colubrids, but is more variable in the point of offset than indicated by both studies. Furthermore, this pattern differs from all of the patterns predicted by Gray and Lissmann (1950).

The lack of correlation between vertebral curvature and the magnitude of muscle activity (Table 2) indicates high variability in curvature or muscular activity patterns. This high variability may reflect variable attenuation of EMG amplitude resulting from different electrode orientations (Loeb and Gans, 1986) or the simultaneous action of other muscles on the vertebral column. Alternatively, a highly variable relationship between muscle activity and kinematics might be expected because unrestrained movement occurs over a low and very small range of the total muscular capacity of the snakes. Similarly, lizards have much greater capacities for force exertion and work than are typically used in locomotion (Farley, 1997).

The experimental addition of mass to a snake increases the drag it must overcome to propel itself and therefore increases the force required for propulsion. In this experiment, the curve around the single peg was always long enough to contain one or more complete epaxial muscle–tendon chains. The significant increases in EMG burst area and duration with the addition of mass indicate that changes in muscle activity are associated with increased force exertion. These results also indicate that much of the force exerted against the peg is produced by the muscles in the bend contacting the peg, rather than by the muscles in distant bends. Although the connective tissues and long tendons of the epaxial muscles may transmit forces along the trunk, in normal movement they probably do not do so beyond the half-wavelength bend around a point of force exertion. However, because the location of external force exertion by the body wall may differ substantially from the points of muscular force exertion on the skeleton (Cundall, 1987), this pattern may differ when very large forces are required.

In the first bend anterior to each point of contact with a peg, the epaxial muscles are usually active at a much lower spike frequency and amplitude than in other bends (Fig. 6). In addition, activity in this bend is often briefly bilateral (Fig. 6). This low-level firing pattern suggests activity of tonic fibers

(see Carrier, 1989), which are common in the axial muscles of snakes (Guthe, 1981). However, with the lower band limits of the preamplifier and digital filter set to 10 Hz, we were unable to detect low-frequency components in the EMG signals that might indicate the activity of tonic fibers. The anomalous pattern of muscle activity in the first bend anterior to the peg supports Gray's (1946) hypothesis that muscle activity anterior to a site of force exertion stiffens, rather than bends, the trunk as it is pushed forward from the site of force exertion.

The epaxial muscles are active in series of 1–25 segments (mean 7.66 segments). There is usually a delay of 0–9 vertebrae (mean 2.75 vertebrae) in the shift of epaxial muscle activity from one side to the other. The number of epaxial muscle segments that are active simultaneously in *Pituophis melanoleucus affinis* is smaller than the range of 30–100 active segments reported for *Elaphe obsoleta* and *Nerodia fasciata* (Jayne, 1988). In contrast to the colubrid pattern, the epaxial muscles of the heavy-bodied *Python regius* are reported to be active in blocks of only 8–10 segments near the peg contact site (Gasc *et al*. 1989). The experimental addition of mass to one gopher snake did not produce the difference in the timing of muscle activity reported between the other slender colubrid snakes (Jayne, 1988; present study) and the stout boid snake (Gasc *et al*. 1989).

Although epaxial muscles generally are not active bilaterally in *Pituophis melanoleucus affinis*, their points of insertion may overlap by 6–22 vertebrae. Consequently, the vertebrae in the zone of overlap are subject to complex torques from the actions of antagonistic contralateral muscles (Gasc *et al*. 1989). The roles of the epaxial muscles are further complicated by their elongate tendons. These long tendons may act as large series elastic components and thus may have complex effects on the moments exerted by the muscles on the skeleton.

The only previously hypothesized function of the long tendons and serial interconnections of snake epaxial muscles is to produce curvature and exert forces over long arcs of the trunk (Mosauer, 1932*a*,*b*; Gans, 1962; Ruben, 1977). However, the anatomy of the epaxial muscle–tendon chains and the timing of epaxial muscle activity suggest several additional functions. (1) The epaxial muscle–tendon system produces complex lateral, vertical and torsional forces over several vertebrae, particularly where the insertions of simultaneously active contralateral muscles overlap. (2) Adjacent muscle segments, with adjacent insertion sites, act in series in shortening but in parallel in force production, thus allowing effective shortening and force production by the elongate muscles. (3) The additive shortening of the serially connected epaxial muscles (SSP–LD and LD–IL) may compensate for elastic stretch in the long tendons. (4) Alternatively, during simultaneous activity, the interconnected IL, LD and SSP segments may constrain one another to isometric activity. If the hypaxial muscles also contribute to axial bending during locomotion, then isometric activity of the epaxial muscles would be consistent with the hypothesis of Rome and Lindstedt (1997) that muscles may be functionally divided into those that produce force isometrically and those that produce work by shortening. (5) The long tendons have larger volumes and therefore slower elastic recoils than would short tendons, which may enhance the recycling of elastic strain energy during the low-frequency undulations of crawling snakes (Alexander, 1988, 1997). (6) The LD is stretched prior to and upon activation by the active SSP and IL segments connected to it anteriorly (Fig. 9). This stretching may activate receptors in the muscles and tendons (reviewed in Guthe, 1981; Crowe, 1992) and thereby increases the force output of the LD (Katz, 1939; Gordon *et al*. 1966; Cavagna *et al*. 1968, 1975; Cavagna and Citterio, 1974).

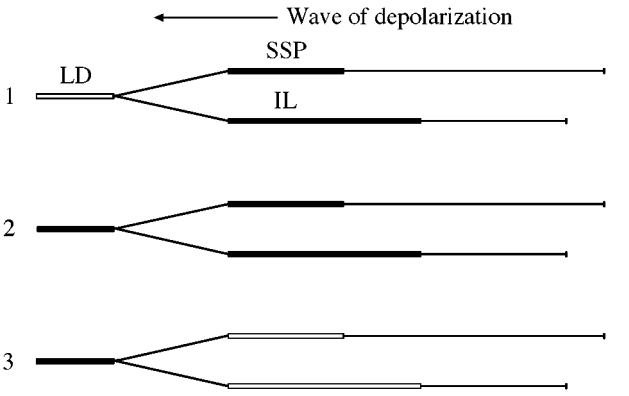

Fig. 9. Schematic diagram of three stages in the propagation of epaxial muscular activity along the body of *Pituophis melanoleucus affinis*. Anterior is to the right. The solid thick bars represent active epaxial muscles, the open thick bars represent inactive muscles and the thin lines represent tendons. At time 1, the M. semispinalis (SSP) and M. iliocostalis (IL) actively pull on the M. longissimus dorsi (LD) prior to and during its activation. At time 2, all three epaxial muscles are active simultaneously. At time 3, the SSP and IL are inactive while the LD remains active. Subsequent to time 3, all three muscles are inactive until the cycle repeats. The physiological and mechanical consequences of this activation pattern are discussed in the text.

Major anatomical differences among lineages of snakes such as boids, colubrids and viperids (Mosauer, 1935; Gasc, 1981) probably have different mechanical effects, particularly those hypothesized in points 3, 4 and 5 above. In addition, even subtle anatomical differences among colubrid species may have important mechanical effects. For example, in many snakes, the tendon connecting SSP and LD segments inserts on the skeleton between these muscles (Gasc, 1981). This insertion may act as a brake on the series elasticity of the epaxial muscle–tendon chain by directing some force to act on the skeleton in the middle of the chain. Although this short tendon appears to be absent in Sonoran gopher snakes, it may be present in snakes from other populations of this variable, widespread species.

These hypotheses encompass both physiological and mechanical effects. However, some of these effects, such as the elastic properties and roles of the complex muscle–tendon chains, are poorly understood. The mechanics of the muscles and tendons, and their relationships with locomotor

kinematics, may be studied in large snakes using established techniques (e.g. Biewener, 1992; Biewener and Full, 1992; Blickhan and Full, 1992).

Propulsion

Muscular activity produces and propagates bends along the trunk (Jayne, 1988; Gasc *et al*. 1989; present study). The pattern of epaxial muscle activity recorded in gopher snakes is consistent with muscular shortening and production of the propulsive bend around the peg, as predicted by Gray (1946) and recorded by Jayne (1988) in other colubrid snakes. Muscle activity contralateral to the point of contact pushes the vertebral column against the peg (Fig. 10; Gray, 1946). Epaxial muscle action over more vertebrae anterior than posterior to the peg causes the vertebral column to bend around the peg and reverse curvature anterior to it. The body wall deforms asymmetrically around the peg, with the sharpest curvature around its anterior surface. This asymmetrical, short-radius deformation of the body wall around each peg appears to be a critical component in both colubrids (Gray, 1946; present study) and boids (e.g. *Python regius*; Gasc *et al*. 1989).

The snake travels forward and exerts force by continuously bending around each point of contact and thus shifting the point of contact to more posterior segments of the body (Gray, 1953*a*; Gasc *et al*. 1989; Gans, 1994; present study). The propulsive mechanism may be modeled as a modified cam-follower system (Fig. 1; Gasc *et al*. 1989; Gans, 1994; Gans *et al*. 1997). A cam mechanism generates translational movement in a follower that is constrained to linear excursion and is spring-loaded to maintain contact with the cam plate. Whenever the cam plate moves, the follower slides or rolls along its curved edge. In a freely rotating cam plate, a follower that is pushed against its edge would be displaced towards the center of rotation of the plate; on a concave arc of the cam plate, this movement would be towards a region of lesser curvature of the plate (Fig. 1).

In the case of a crawling snake, the curved trunk represents an arc of the cam plate, the peg represents a fixed follower, and the equivalent of the spring loading is due to the force exerted by the body against the peg (Fig. 10). Hence, the point of contact between the concave body wall and the peg will be displaced from a region of greater curvature (which occurs around the anterior surface of the peg) to a region of lesser curvature (posterior to the peg). Progression (translation) results from continuous bending (rotation) of successive segments of the snake body around the peg. The extent of bending around a peg and the degree of curvature reversal control the direction of force exertion and movement (Gasc *et al*. 1989).

Propulsion of the snake-like robot constructed by Hirose (1993) appears to be based on this kind of cam-follower mechanism. However, the bending pattern of the robot does not involve local deformation of the body surface around points of force exertion, which is an important element of the propulsive mechanism in snakes.

Propulsive contact between the trunk and a peg requires a high degree of sensory–motor coordination (Gans, 1985). The body wall has to be deformed so that the portion immediately anterior to the peg always has a greater curvature than the portion posterior to it. This postural adjustment involves differential movement of the vertebral column and body wall. In snakes, as in the snake-like robots designed by Hirose (1993), deformation of the body around a peg minimally requires propagation of motor output, acute sensory feedback and lateral inhibition. The coordination required to maintain multiple points in contact with multiple pegs, and to propagate these points along the trunk, is even greater. Our observations of newly hatched gopher snakes (*Pituophis melanoleucus affinis*), king snakes (*Lampropeltis getula*) and racers (*Coluber constrictor*) indicate that even these are fully capable of effective lateral undulation, and hence cam propulsion, against single or multiple pegs.

Gray (1946, p. 119) and Gans (1970, 1974) argued that terrestrial lateral undulation in snakes requires at least three points of simultaneous contact to cancel opposing lateral force vectors. For this reason, Gasc *et al*. (1989) argued that locomotion in *Python regius* pushing against a single peg is not lateral undulation. Our current results indicate that the cam-follower mechanism can apply to any number of contact points. Consequently, although the kinematics of locomotion against a single peg may differ from that of typical lateral

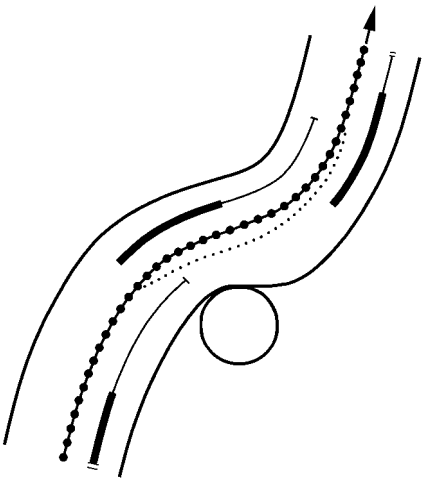

Fig. 10. Schematic drawing of epaxial muscle activity and its action on vertebral curvature in *Pituophis melanoleucus affinis* pushing against one of several pegs with which it is in contact. Muscle activity contralateral to the peg pushes the vertebral column against it. Action of the muscles over more vertebrae anterior than posterior to the peg causes the trunk to bend around and reverse curvature anterior to the peg. Note the zones of torque in which the insertions of active muscles on one side overlap with the active muscle segments on the other side. The arrow indicates the direction of travel. The thick line indicates epaxial muscle activity and the thin lines indicate the anterior tendons of the active muscles. The large dots along the midline indicate vertebrae and the dotted line indicates the tendency of the vertebral column to bend under the action of the epaxial muscles.

undulation (Fig. 3), the propulsive mechanism at each point of contact appears to be the same.

Although multiple sites of propulsive contact are not required for effective locomotion, contact with multiple pegs involves two important elements that enhance the effectiveness of terrestrial lateral undulation. The first is that contact with multiple pegs allows cancellation of lateral force vectors over an extended length of the trunk, which stabilizes the body against lateral slippage (Mosauer, 1932*a*,*b*; Gray, 1946; Gray and Lissmann, 1950; Gans, 1962). The second is that contact with multiple pegs allows for lower curvature around each peg, which may be related to locomotor speed (Ruben, 1977). These two effects appear to facilitate higher speed, with less lateral slippage, in lateral undulation through a field of pegs than by pushing against only one or two pegs. In addition to the number of pegs contacted simultaneously, the peg spacing relative to snake size has important effects on locomotor kinematics (Bennet *et al*. 1974).

The cam-follower model leads to two predictions. (1) Muscular activity is correlated with local curvature of the vertebral midline or body wall because axial bending is produced by sequential active bending of each segment of the trunk. In our sample, curvature of the body wall is significantly greater around the anterior surface than around the posterior surface of the peg. In addition, vertebral curvature and EMG burst area increase whenever the drag of a snake increases substantially. (2) The degree of curvature around each peg should be modulated to accommodate requirements for force exertion. This prediction is consistent with the results of Gasc *et al*. (1989) for *Python regius*. A corollary of this hypothesis is that the degree of curvature around each peg should be related inversely to the number of pegs contacted simultaneously. This prediction appears to be consistent with the results of Gray and Lissmann (1950) for *Natrix* (*Tropidonotus*) *natrix*, although curvature was not quantified in that study. These hypotheses are supported by the qualitative patterns exhibited by gopher snakes, although they require quantitative tests.

The key mechanical features of terrestrial lateral undulation are long-radius curvature of the vertebral column around each peg and short-radius asymmetric curvature of the body wall around the peg. The long-radius vertebral bends around resistance sites involve complex lateral and torsional movements and appear to be produced largely by the epaxial musculature, although other muscles may have important mechanical effects. The short-radius curvature of the body wall around the anterior surface of each resistance site appears to result from a combination of vertebral curvature, axial torsion and movement of the ribs and body wall. Local movement of the body wall may be produced by hypaxial muscles that act on the ribs and skin, as in *Python regius* (Gasc *et al*. 1989). Also critical is the sensory–motor coordination that allows the snake to maintain and propagate zones of contact with one or more pegs, even when the head and tail undergo considerable lateral slippage. Some of these elements were noted in the early literature (e.g. Stradling, 1882; Fokker, 1927; Van Leeuwen, 1927; Mosauer, 1932*a*,*b*; Gray, 1946, 1953*b*; Gans, 1962), but had not previously been synthesized into a detailed mechanical model of the propulsive mechanism.

Evolutionary patterns

The role of epaxial muscles in producing axial bends appears to be a derived feature of snakes relative to quadrupedal lizards, in which the epaxial muscles do not appear to contribute to lateral bending during locomotion (Ritter, 1995, 1996). Furthermore, the capacity of snakes to maintain one or more sites of contact for the entire length of the trunk exceeds that of most limbless lizards, which have not been reported to exhibit differential curvature of the vertebral column and body wall and which slip continuously into and out of contact with external objects (Gans, 1985, 1986, 1994). The latter features led Gans (1985, 1986, 1994) to describe the undulatory locomotion of most limbless lizards as ‘simple undulation’ to distinguish it from the more complex terrestrial ‘lateral undulation’ of snakes. Terrestrial lateral undulation in snakes involves a unique propulsive mechanism that is highly derived relative to both aquatic undulation and the terrestrial ‘simple undulation’ of other squamates.

This research was approved by the University Committee on the Use and Care of Animals at The University of Michigan. We are indebted to George Ferguson, George Good, Cecil Schwalbe and Tom Taylor for donation of the animals used in various stages of this study and to Katherine Wadsworth and Paul Webb for valuable statistical advice. Jennifer Ast, Jean-Pierre Gasc and Tom Daniel provided valuable input, and Jean-Pierre Gasc kindly allowed us to indicate the original source of the cam-follower idea. Thanks also to Jules Villareal and Jason Laczko for help with experiments and preliminary analyses, respectively. The University of Michigan Media Services lent us the video camera. This research was funded in part by the Department of Biology and Rackham Graduate School of The University of Michigan, The University of Arizona Graduate School and the Leo Leeser Fund. The Department of Biology and Rackham Graduate School of The University of Michigan supported presentation of this project at the Fourth and Fifth International Congresses of Vertebrate Morphology. An NSF Travel Grant, awarded to B.R.M. through the Herpetologists’ League and the Society for the Study of Amphibians and Reptiles, supported presentation of part of this work at the Third World Congress of Herpetology.

References

ALEXANDER, A. A. AND GANS, C. (1966). The pattern of dermal–vertebral correlation in snakes and amphisbaenians. *Zool. Meded.* **41**, 171–190.

ALEXANDER, R. MCN. (1988). *Elastic Mechanisms in Animal Movement*. Cambridge: Cambridge University Press.

ALEXANDER, R. MCN. (1997). Optimum muscle design for oscillatory movements. *J. theor. Biol.* **184**, 253–259.

BENNET, S., MCCONNELL, T. AND TRUBATCH, S. L. (1974). Quantitative analysis of the speed of snakes as a function of peg spacing. *J. exp. Biol.* **60**, 161–165.

BENNETT, R. A. (1996). Anesthesia. In *Reptile Medicine and Surgery* (ed. D. R. Mader), pp. 241–247. Philadelphia, PA: W. B. Saunders Co.

BIEWENER, A. A. (1992). *In vivo* measurement of bone strain and tendon force. In *Biomechanics: Structures and Systems* (ed. A. A. Biewener), pp. 123–147. Oxford: IRL Press.

BIEWENER, A. A. AND FULL, R. J. (1992). Force platform and kinematic analysis. In *Biomechanics: Structures and Systems* (ed. A. A. Biewener), pp. 45–73. Oxford: IRL Press.

BLICKHAN, R. AND FULL, R. J. (1992). Mechanical work in terrestrial locomotion. In *Biomechanics: Structures and Systems* (ed. A. A. Biewener), pp. 75–96. Oxford: IRL Press.

CARRIER, D. (1989). Ventilatory action of the hypaxial muscles of the lizard *Iguana iguana*: a function of slow muscle. *J. exp. Biol.* **143**, 435–457.

CAVAGNA, G. A. AND CITTERIO, G. (1974). Effect of stretching on the elastic characteristics and the contractile component of frog striated muscle. *J. Physiol., Lond.* **239**, 1–14.

CAVAGNA, G. A., CITTERIO, G. AND JACINI, P. (1975). The additional mechanical energy delivered by the contractile component of the previously stretched muscle. *Proc. physiol. Soc.* **1975**, 65–66.

CAVAGNA, G. A., DUSMAN, B. AND MARGARIA, R. (1968). Positive work done by a previously stretched muscle. *J. appl. Physiol.* **24**, 21–32.

CROWE, A. (1992). Muscle spindles, tendon organs and joint receptors. In *Biology of the Reptilia*, vol. 17 (ed. C. Gans and P. S. Ulinski), pp. 454–495. Chicago, IL: University Chicago Press.

CUNDALL, D. (1987). Functional morphology. In *Snakes: Ecology and Evolutionary Biology* (ed. R. A. Seigel, J. T. Collins and S. S. Novak), pp. 106–140. New York: McGraw-Hill.

FARLEY, C. T. (1997). Maximum speed and mechanical power output in lizards. *J. exp. Biol.* **200**, 2189–2195.

FOKKER, A. D. (1927). De Voortbeweging der slangen. *Physica* **7**, 65–71.

GANS, C. (1962). Terrestrial locomotion without limbs. *Am. Zool.* **2**, 167–182.

GANS, C. (1970). How snakes move. *Scient. Am.* **222**, 82–96.

GANS, C. (1974). *Biomechanics: An Approach to Vertebrate Biology*. New York: Lippincott.

GANS, C. (1984). Slide-pushing: a transitional locomotor method of elongate squamates. *Symp. zool. Soc. Lond.* **52**, 12–26.

GANS, C. (1985). Motor coordination factors in the transition from tetrapody to limblessness in lower vertebrates. In *Coordination of Motor Behaviour* (ed. B. M. H. Bush and F. Clarac). *Soc. exp. Biol. Sem. Ser.* **24**, 183–200.

GANS, C. (1986). Locomotion of limbless vertebrates: pattern and evolution. *Herpetologica* **42**, 33–46.

GANS, C. (1994). Approaches to the evolution of limbless locomotion. *Cuad. Herpetol.* **8**, 12–17.

GANS, C., GAUNT, A. S. AND WEBB, P. W. (1997). Vertebrate locomotion. In *Handbook of Physiology: Comparative Physiology*, section 13, vol. 1 (ed. W. H. Dantzler), pp. 55–213. Oxford: Oxford University Press.

GANS, C. AND MENDELSSOHN, H. (1972). Sidewinding and jumping progression of vipers. In *Toxins of Animal and Plant Origin* (ed. A. de Vries and E. Kochva), pp. 17–38. London: Gordon & Breach Science Publications.

GASC, J.-P. (1967). Retentissement de l'adaptation à la locomotion apode sur le squelette des squamates. In *Problèmes Actuels de Palèontologie: Evolution des Vertébrés* (ed. J.-P. Lehman). *Colloques int. cent. natn Res. Scient.* **163**, 373–394.

GASC, J.-P. (1974). L'interprétation fonctionnelle de l'appareil musculo-squelettique de l'axe vertébral chez les Serpents (Reptilia). *Mém. Mus. Hist. nat. Paris A Zool.* **83**, 1–182.

GASC, J.-P. (1976). Snake vertebrae – a mechanism or merely a taxonomist's toy? In *Morphology and Biology of Reptiles* (ed. A. d'A. Bellairs and C. B. Cox). *Linn. Soc. Symp. Ser.* **3**, 177–190.

GASC, J.-P. (1981). Axial musculature. In *Biology of the Reptilia*, vol. 11 (ed. C. Gans and T. S. Parsons), pp. 355–435. New York: Academic Press.

GASC, J.-P., CATTAERT, D., CHASSERAT, C. AND CLARAC, F. (1989). Propulsive action of a snake pushing against a single site: its combined analysis. *J. Morph.* **201**, 315–329.

GORDON, A. M., HUXLEY, A. F. AND JULIAN, F. J. (1966). The variation in isometric tension with sarcomere length in vertebrate muscle fibres. *J. Physiol., Lond.* **184**, 170–192.

GRAY, J. (1946). The mechanism of locomotion in snakes. *J. exp. Biol.* **23**, 101–120.

GRAY, J. (1953*a*). *How Animals Move*. Cambridge: Cambridge University Press.

GRAY, J. (1953*b*). Undulatory propulsion. *Q. J. microsc. Sci.* **94**, 551–578.

GRAY, J. AND LISSMANN, H. W. (1950). The kinetics of locomotion of the grass-snake. *J. exp. Biol.* **26**, 354–367.

GUTHE, K. F. (1981). Reptilian muscle: fine structure and physiological parameters. In *Biology of the Reptilia*, vol. 11 (ed. C. Gans and T. S. Parsons), pp. 265–354. New York: Academic Press.

HIROSE, S. (1993). *Biologically Inspired Robots: Snake-like Locomotors and Manipulators*. Oxford: Oxford University Press.

JAYNE, B. C. (1982). Comparative morphology of the semispinalis-spinalis muscle of snakes and correlations with locomotion and constriction. *J. Morph.* **172**, 83–96.

JAYNE, B. C. (1988). Muscular mechanisms of snake locomotion: an electromyographic study of lateral undulation of the Florida banded water snake (*Nerodia fasciata*) and the yellow rat snake (*Elaphe obsoleta*). *J. Morph.* **197**, 159–181.

JAYNE, B. C., LAUDER, G. V., REILLY, S. M. AND WAINWRIGHT, P. C. (1990). The effect of sampling rate on the analysis of digital electromyograms from vertebrate muscle. *J. exp. Biol.* **154**, 557–565.

KATZ, B. (1939). The relation between force and speed in muscular contraction. *J. Physiol., Lond.* **96**, 45–64.

LOEB, G. E. AND GANS, C. (1986). *Electromyography for Experimentalists*. Chicago, IL: University of Chicago Press.

MOON, B. R. (1996). Sampling rates, aliasing and the analysis of electrophysiological signals. In *Proceedings of the 15th Southern Biomedical Engineering Conference* (ed. P. K. Bajpai), pp. 401–404. Piscataway, NJ: IEEE Service Center.

MOSAUER, W. (1932*a*). On the locomotion of snakes. *Science* **76**, 583–585.

MOSAUER, W. (1932*b*). Über die Ortsbewegung der Schlangen: Eine Kritik und Ergänzung der Arbeit Wiedemann's. *Zool. Jb. (Zool.)* **52**, 191–215.

MOSAUER, W. (1935). The myology of the trunk region of snakes and its significance for ophidian taxonomy and phylogeny. *Univ. Calif. Publ. biol. Sci.* **1**, 81–120.

OSTROWSKI, J. AND BURDICK, J. (1996). Gait kinematics for a serpentine robot. *Proceedings of the IEEE International Conference on Robotics and Automation* **2**, 1294–1299.

PACKARD, G. C. AND BOARDMAN, T. J. (1987). The misuse of ratios

to scale physiological data that vary allometrically with body size. In *New Directions in Ecological Physiology* (ed. M. E. Feder, A. F. Bennett, W. Burggren and R. B. Huey), pp. 216–239. Cambridge: Cambridge University Press.

PREGILL, G. K. (1977). Axial myology of the racer *Coluber constrictor* with emphasis on the neck region. *Trans. San Diego Soc. nat. Hist.* **18**, 185–206.

PROSKE, U. (1969). Vibration-sensitive mechanoreceptors in snake skin. *Exp. Neurol.* **23**, 187–194.

RITTER, D. (1995). Epaxial muscle function during locomotion in a lizard (*Varanus salvator*) and the proposal of a key innovation in the vertebrate axial musculoskeletal system. *J. exp. Biol.* **198**, 2477–2490.

RITTER, D. (1996). Axial muscle function during lizard locomotion. *J. exp. Biol.* **199**, 2499–2510.

ROME, L. C. AND LINDSTEDT, S. L. (1997). Mechanical and metabolic design of the muscular system in vertebrates. In *Handbook of Physiology: Comparative Physiology*, section 13, vol. 1 (ed. W. H. Dantzler), pp. 1587–1651. Oxford: Oxford University Press.

RUBEN, J. A. (1977). Morphological correlates of predatory modes in the coachwhip (*Masticophis flagellum*) and rosy boa (*Lichanura roseofusca*). *Herpetologica* **33**, 1–6.

STRADLING, A. (1882). Notes about snakes. *Nature* **25**, 377–378.

VAN LEEUWEN, H. J. (1927). De Voortbeweging der Slangen. *Physica* **7**, 119–121.

WIEDEMANN, E. (1932). Zur Ortsbewegung der Schlangen und Schleichen. *Zool. Jb. Allg. (Zool.)* **50**, 557–596.

ZAR, J. H. (1984). *Biostatistical Analysis*, 2nd edn. Englewood Cliffs, NJ: Prentice-Hall.